Intrinsic phasing of heterodyne-detected multidimensional infrared spectra

Johnson, Philip J M ; Koziol, Klemens L ; Hamm, Peter

Abstract: We show that it is possible to phase multidimensional infrared spectra generated by a boxcars geometry four-wave mixing spectrometer directly from the signal generated by the molecular vibration of interest, without the need for auxiliary phasing measurements. For isolated vibrations, the phase profile of the 2D response smoothly varies between fixed phase limits, allowing for a general target for phasing independent of the degree of anharmonicity exhibited between the ground and excited state. As a proof of principle, the 2D response of the similar to 2155 cm(-1) thiocyanate stretch vibration of MeSCN, a system exhibiting anharmonicity such that the 0-1 and 1-2 transitions are spectrally isolated, is successfuly phased directly from the experimental spectra. The methodology is also applied to correctly phase extremely weak signals of the unnatural amino acid azidohomoalanine following background subtraction.

DOI: https://doi.org/10.1364/OE.25.002928

Research Article | Vol. 25, No. 3 | 6 Feb 2017 | OPTICS EXPRESS 2928

Optics EXPRESS

Intrinsic phasing of heterodyne-detected multidimensional infrared spectra

PHILIP J. M. JOHNSON, KLEMENS L. KOZIOL, AND PETER HAMM*

Department of Chemistry, University of Zurich, Winterthurerstrasse 190, CH-8057 Zurich, Switzerland
**peter.hamm@chem.uzh.ch*

Abstract: We show that it is possible to phase multidimensional infrared spectra generated by a boxcars geometry four-wave mixing spectrometer directly from the signal generated by the molecular vibration of interest, without the need for auxiliary phasing measurements. For isolated vibrations, the phase profile of the 2D response smoothly varies between fixed phase limits, allowing for a general target for phasing independent of the degree of anharmonicity exhibited between the ground and excited state. As a proof of principle, the 2D response of the ~2155 cm^{-1} thiocyanate stretch vibration of MeSCN, a system exhibiting anharmonicity such that the 0–1 and 1–2 transitions are spectrally isolated, is successfuly phased directly from the experimental spectra. The methodology is also applied to correctly phase extremely weak signals of the unnatural amino acid azidohomoalanine following background subtraction.

OCIS codes: (300.6290) Spectroscopy, four-wave mixing; (300.6300) Spectroscopy, Fourier transforms; (300.6310) Spectroscopy, heterodyne; (300.6340) Spectroscopy, infrared; (320.7150) Ultrafast spectroscopy.

References and links

1. P. Hamm and M. Zanni, *Concepts and Methods of 2D Infrared Spectroscopy* (Cambridge University, 2011).
2. M. Khalil, N. Demirdöven, and A. Tokmakoff, "Obtaining Absorptive Line Shapes in Two-Dimensional Infrared Vibrational Correlation Spectra," Phys. Rev. Lett. **90**, 047401 (2003).
3. S. M. Gallagher Faeder and D. M. Jonas, "Two-Dimensional Electronic Correlation and Relaxation Spectra: Theory and Model Calculations," J. Phys. Chem. A **103**, 10489–10505 (1999).
4. V. I. Prokhorenko, A. Halpin, and R. J. D. Miller, "Coherently-controlled two-dimensional photon echo electronic spectroscopy," Opt. Express **17**, 9764–9779 (2009).
5. F. Milota, C. N. Lincoln, and J. Hauer, "Precise phasing of 2D-electronic spectra in a fully non-collinear phase-matching geometry," Opt. Express **21**, 15904–15911 (2013).
6. A. D. Brisow, D. Karaiskaj, X. Dai, and S. T. Cundiff, "All-optical retrieval of the global phase for two-dimensional Fourier-transform spectroscopy," Opt. Express **16**, 18017–18027 (2008).
7. E. H. G. Backus, S. Garrett-Roe, and P. Hamm, "Phasing problem of heterodyne-detected two-dimensional infrared spectroscopy," Opt. Lett. **33**, 2665–2667 (2008).
8. D. B. Turner, K. E. Wilk, P. M. G. Curmi, G. D. Scholes, "Comparison of Electronic and Vibrational Coherence Measured by Two-Dimensional Electronic Spectroscopy," J. Phys. Chem. Lett. **2**, 1904–1911 (2011).
9. J. Helbing and P. Hamm, "Compact implementation of Fourier transform two-dimensional IR spectroscopy without phase ambiguity," J. Opt. Soc. Am. B **28**, 171–178 (2011).
10. Y. Zhang, T.-M. Yan, and Y. H. Jiang, "Precise phase determination with the built-in spectral interferometry in two-dimensional electronic spectroscopy," Opt. Lett. **41**, 4134–4137 (2016).
11. W. Rock, Y.-L. Li, P. Pagano, and C. M. Cheatum, "2D IR spectroscopy using Four-Wave Mixing, Pulse Shaping, and IR Upconversion: A Quantitative Comparison," J. Phys. Chem. A **117**, 6073–6083 (2013).
12. P. Hamm, M. Lim, R. H. Hochstrasser, "Structure of the Amide I Band of Peptides Measured by Femtosecond Nonlinear-Infrared Spectroscopy," J. Phys. Chem. B **102,** 6123–6138 (1998).
13. V. Volkov, R. Schanz, and P. Hamm, "Active phase stabilization in Fourier-transform two-dimensional infrared spectroscopy," Opt. Lett. **30**, 2010–2012 (2005).
14. R. Bloem, K. Koziol, S. A. Waldauer, B. Buchli, R. Walser, B. Samatanga, I. Jelesarov, and P. Hamm, "Ligand Binding Studied by 2D IR Spectroscopy Using the Azidohomoalanine Label," J. Phys. Chem. B **116**, 13705–13712 (2012).
15. P. Hamm, R. A. Kaindl, and J. Stenger, "Noise suppression in femtosecond mid-infrared light sources," Opt. Lett. **25**, 1798–1800 (2000).
16. R. Bloem, S. Garrett-Roe, H. Strzalka, P. Hamm, and P. Donaldson, "Enhancing signal detection and completely eliminating scattering using quasi-phase-cycling in 2D IR experiments," Opt. Express **18**, 27067–27078 (2010).
17. C. Dorrer, N. Belabas, J.-P. Likforman, and M. Joffre, "Spectral resolution and sampling issues in Fourier-transform spectral interferometry," J. Opt. Soc. Am. B **17**, 1795–1802 (2000).

#282092 https://doi.org/10.1364/OE.25.002928
Journal © 2017 Received 2 Dec 2016; revised 16 Jan 2017; accepted 27 Jan 2017; published 3 Feb 2017

Optics EXPRESS

18. S. T. Roberts, J. J. Loparo, and A. Tokmakoff, "Characterization of spectral diffusion from two-dimensional line shapes," J. Chem. Phys. **125**, 084502 (2006).
19. A. Nemeth, F. Milota, T. Mančal, V. Lukeš, J. Hauer, H. F. Kauffmann, and J. Sperling, "Vibrational wave packet induced oscillations in two-dimensional electronic spectra. I. Experiments," J. Chem. Phys. **132**, 184514 (2010).
20. H. Taskent-Sezgin, J. Chung, P. S. Banerjee, S. Nagarajan, R. B. Dyer, I. Carrico, and D. P. Raleigh, "Azidohomoalanine: A Conformationally Sensitive IR Probe of Protein Folding, Protein Structure, and Electrostatics," Angew. Chem. Int. Ed. **49**, 7473–7475 (2010).
21. J. K. Chung, M. C. Thielges, and M. D. Fayer, "Conformational Dynamics and Stability of HP35 Studied with 2D IR Vibrational Echoes," J. Am. Chem. Soc. **134**, 12118–12124 (2012).
22. M. M. Waegele, R. M. Culik, and F. Gai, "Site-Specific Spectroscopic Reporters of the Local Electric Field, Hydrations, Structure, and Dynamics of Biomolecules," J. Phys. Chem. Lett. **2**, 2598–2609 (2011).
23. J.-J. Max and C. Chapados, "Isotope effects in liquid water by infrared spectroscopy. III. H_2O and D_2O spectra from 6000 to 0 cm^{-1}," J. Chem. Phys. **131**, 184505 (2009).
24. K. L. Koziol, P. J. M. Johnson, S. Stucki-Buchli, S. A. Waldauer, and P. Hamm, "Fast infrared spectroscopy of protein dynamics: advancing sensitivity and selectivity," Curr. Opin. Struct. Biol. **34**, 1–6 (2015).
25. L. De Marco, W. Carpenter, H. Liu, R. Biswas, J. M. Bowman, and A. Tokmakoff, "Differences in the Vibrational Dynamics of H2O and D2O: Observation of Symmetric and Antisymmetric Stretching Vibrations in Heavy Water," J. Phys. Chem. Lett. **7**, 1769–1774 (2016).
26. K. Ramasesha, L. De Marco, A. Mandal, and A. Tokmakoff, "Water vibrations have strongly mixed intra- and intermolecular character," Nat. Chem. **5**, 935–940 (2013).
27. S.-H. Shim, D. B. Strasfeld, Y. L. Ling, and M. T. Zanni, "Automated 2D IR spectroscopy using a mid-IR pulse shaper and application of this technology to the human islet amyloid polypeptide," Proc. Natl. Acad. Sci. USA **104**, 14197–14202 (2007).
28. L. P. DeFlores, R. A. Nicodemus, and A. Tokmakoff, "Two-dimensional Fourier transform spectroscopy in the pump-probe geometry," Opt. Lett. **32**, 2966–2968 (2007).
29. S.-H. Shim and M. T. Zanni, "How to turn your pump-probe instrument into a multidimensional spectrometer: 2D IR and Vis spectroscopies *via* pulse shaping," Phys. Chem. Chem. Phys. **11**, 748–761 (2009).

1. Introduction

Two-dimensional infrared spectroscopy measures the correlation of the third order vibrational response of a system to the excitation fields, allowing for greater insight into such diverse processes as solvent fluctuations, electron transfer processes, and protein folding or dynamics [1]. Heterodyne detection is typically employed to both amplify the weak emitted signal fields and to allow for isolation of the purely absorptive and dispersive contributions to the third order response [2], wherein the weak signal field is mixed with a large local oscillator (LO) on the detector and the interferogram between the two is measured. The purely absorptive response can be isolated only through precise knowledge of the relative timing and phases of the electric fields which generate the heterodyne signal.

A number of methods for this *phasing* of heterodyne-detected multidimensional spectra have been proposed. Comparative methods use the equivalence of all four-wave mixing signals to allow for a projection-slice comparison of the heterodyne-detected multidimensional spectrum to the pump-probe [3, 4] or transient grating [5] response at the equivalent waiting time. Interferometric methods, alternatively, measure the relative phases of the pulse pairs which generate the heterodyne signal directly from interferograms of the excitation pulses themselves, either spatially [6, 7] or spectrally [8]. The spatial interferogram technique was shown to be applicable in the IR in the limiting case of thin samples (~5 μm, where the scattering source has the same dimensions as the sample thickness), but fails for thicker samples where deviations from the idealized boxcar geometry rapidly introduce systematic errors in phasing [7]. Collinear geometry 2D IR setups have largely solved the phasing problem [9], but as boxcar geometry 2D IR instruments allow for the highest possible sensitivity, a reliable and robust method for phasing, particularly in the limiting case of low concentrations and weak signal magnitudes where comparative methods fail, is still in demand.

In most of the above cases, the phasing methodology relies on the long-term phase stability of the interferometer, and it must be assumed that the phase does not drift following the phasing procedure. A more advantageous method would be to recover the global phase offset from the

Optics EXPRESS

heterodyne interferograms of the system response directly. Such an approach would obviate the need for auxiliary phasing procedures and allow for even greater insensitivity to long-term drifts of the interferometer (a recent paper proposes an approach based on spectral interferometry for phasing multidimensional electronic spectroscopy [10], which is applicable in the limiting case of sufficiently long waiting times such that the rephasing and nonrephasing response are symmetric). The interferograms generated by the system response contain the phase offset of the heterodyne signal that must be corrected, arising from the imperfect knowledge and control of the relative timing and phase profiles of the excitation pulses used to generate and detect the four-wave mixing signal. Provided that the phase profile of the 2D IR response of the vibrational transition under study is known, it should be possible to recover the global phase offset directly from the argument of the Fourier transform of the coherence time interferograms.

While this initially may appear as a significant restriction, that of knowing *a priori* what the purely absorptive 2D IR spectrum should look like, here we show that general features of the two-dimensional response of isolated vibrations with and without significant anharmonicity between the ground and excited state show a consistent phase progression between fixed phase limits, giving a general target for phasing of isolated peaks or even strongly overlapping ground and excited state transitions. Comparison of the simulated phase response with experiments on MeSCN in dimethylformamide (DMF), exciting the thiocyanate stretch vibration at 2155 cm^{-1} [11], represent a proof of principle example of this approach. We then apply this methodology to correctly phase the weak response of the azido stretch group of the unnatural amino acid azidohomoalanine in D_2O based solvent, allowing for the correct phasing of extremely weak signals buried in strong solvent backgrounds.

2. Methods and materials

2.1. Simulations

Using the standard response function formalism [1], the two-dimensional response of a vibration up to the the second excited state was calculated in the impulsive limit, employing the Condon approximation and the cumulant expansion up to second order. The rephasing and non-rephasing response functions in the time domain take the form

$$\begin{aligned} R_R &= \mu^4 \left(e^{-i((\omega_{01}-\Delta)t_3-\omega_{01}t_1)} - e^{-i\omega_{01}(t_3-t_1)}\right) e^{-g(t_1)+g(t_2)-g(t_3)-g(t_1+t_2)-g(t_2+t_3)+g(t_1+t_2+t_3)} \\ R_{NR} &= \mu^4 \left(e^{-i((\omega_{01}-\Delta)t_3+\omega_{01}t_1)} - e^{-i\omega_{01}(t_3+t_1)}\right) e^{-g(t_1)-g(t_2)-g(t_3)+g(t_1+t_2)+g(t_2+t_3)-g(t_1+t_2+t_3)} \end{aligned} \quad (1)$$

for transition dipole moment μ (we set both the 0–1 and 1–2 signals to have the same amplitude), coherence times t_1 and t_3, population time t_2, and lineshape function $g(t)$. With a central frequency of the $0 \rightarrow 1$ transition of $\omega_{01} = 2155$ cm^{-1}, a Kubo lineshape function

$$g(t) = \Delta\omega^2\tau_c^2\left[e^{-t/\tau_c} + \frac{t}{\tau_c} - 1\right], \quad (2)$$

with a fluctuation amplitude ($\Delta\omega$) of 0.1 ps^{-1} and a correlation time (τ_c) of 1.5 ps gives a reasonable approximation of the lineshape of the thiocyanate stretch of MeSCN in DMF [11]. The anharmonicity between the ground and excited state ($\Delta = \omega_{01} - \omega_{12}$) was varied in factors of ten from 2.5 cm^{-1} to 250 cm^{-1} to investigate the effect of overlapping ground and excited state features on the phase profiles of the multidimensional response. The rephasing and non-rephasing response in the frequency domain result following Fourier transformation about both coherence times,

$$\begin{aligned} S_R(\omega_1, t_2, \omega_3) &= \int_0^\infty \int_0^\infty R_R e^{i\omega_1 t_1} e^{i\omega_3 t_3} dt_1 dt_3 \\ S_{NR}(\omega_1, t_2, \omega_3) &= \int_0^\infty \int_0^\infty R_{NR} e^{i\omega_1 t_1} e^{i\omega_3 t_3} dt_1 dt_3, \end{aligned} \quad (3)$$

Optics EXPRESS

where the purely absorptive 2D IR spectrum, $S_A(\omega_1, t_2, \omega_3)$, is calculated by taking the real part of the sum of the rephasing and nonrephasing contributions, following appropriate inversion of ω_1:

$$S_A(\omega_1, t_2, \omega_3) = \Re[S_R(-\omega_1, t_2, \omega_3) + S_{NR}(\omega_1, t_2, \omega_3)]. \quad (4)$$

By convention, we set the bleach to be negative in amplitude, in conjunction with the pump-probe origins of the 2D IR technique [12]. In addition to the purely absorptive spectrum, the phase spectrum, $S_P(\omega_1, t_2, \omega_3)$, of the 2D signals can also be recovered taking the argument of the complex valued 2D response in a similar manner:

$$S_P(\omega_1, t_2, \omega_3) = \mathrm{Arg}[S_R(-\omega_1, t_2, \omega_3) + S_{NR}(\omega_1, t_2, \omega_3)]. \quad (5)$$

2.2. Experimental methods

The boxcars geometry 2D IR spectrometer is the evolution of previously described instrumentation [13, 14]. Mid-infrared light is generated in a home built OPA [15] providing 150 fs FWHM, ~2 μJ pulses centered at the frequency of the vibrational transition of interest at a repetition rate of 5 kHz. The mid IR beam is subsequently split into three equally intense pulses by custom dielectric BaF_2 beamsplitters, while a Fresnel reflection of beam 3 is used for creation of the LO. Fast mechanical scanning of the coherence time delays (beams 1 and 2) is realized by voice coil stages (Equipment Solutions, USA) which translate in a continuous manner to maximize the duty cycle of signal collection and at a rate which roughly samples at the Nyquist frequency of the mid IR fringe. As a result of the continuous scanning nature of the voice coil stages, co-propagating HeNe beams (Melles Griot, USA) are employed for interferometric tracking of the coherence time delay, allowing for binning at a resolution of ~2.11 fs. This results in greater than seven bins per mid IR fringe, significantly oversampling the heterodyne-detected interferograms. Quasi phase-cycling through waiting time modulation of $\pm\pi/2$ steps for each subsequent laser shot by a photoelastic modulator (Hinds Instruments, USA) provides scatter suppression [16]. The signals are detected with a 2×32 pixel MCT array detector (Infrared Associates, USA) operating in a balanced detection scheme which inherently subtracts the static LO contribution. A 300 groove/mm grating blazed at 4 μm (HORIBA Scientific, France) provides ~2.3 cm^{-1} resolution along the detection axis.

Initial zeroing of the pulse delays was realized by spectral interferometry [17]. Briefly, a 10 μm pinhole at the sample position was used as a scattering source, and the fringe spacing in the spectral interferograms generated by each pulse paired with the static beam 3 was used to determine the zero delays. As the amplitude of the scattered light from the LO is significantly weaker than with beams 1 and 2, the zero delays were confirmed with the temporal interferograms of the spectrally-integrated pulses, as described previously [7]. Following this procedure, the pinhole was replaced by a sample cell composed of two CaF_2 windows (2 mm thickness) and a teflon spacer (25 μm thickness) containing either a 100 mM solution of MeSCN in DMF, 100 μM azidohomoalanine in D_2O buffer (50 mM borate, 150 mM NaCl, pH 8.5 buffer), or a D_2O buffer blank (chemicals were purchased from Sigma-Aldrich, except for azidohomoalanine which was purchased from Bachem AG, and were used as received). Rephasing and nonrephasing multidimensional spectra were then measured successively over a total coherence time (t_1) domain of [-5.170, 5.170] ps, in ~2.11 fs bins, resulting in an excitation frequency resolution of ~3.2 cm^{-1}. The experimental 2D spectra were interpolated to yield 32×32 arrays equally spaced in the frequency domain, with the frequency range determined by the spectrometer calibration.

3. Results & discussion

3.1. Simulations

Simulated purely absorptive 2D IR and associated phase spectra at a waiting time of t_2 = 250 fs are shown in Fig. 1 for anharmonicities of (a) 250 cm^{-1}, (b) 25 cm^{-1}, and (c) 2.5 cm^{-1}, where

Optics EXPRESS

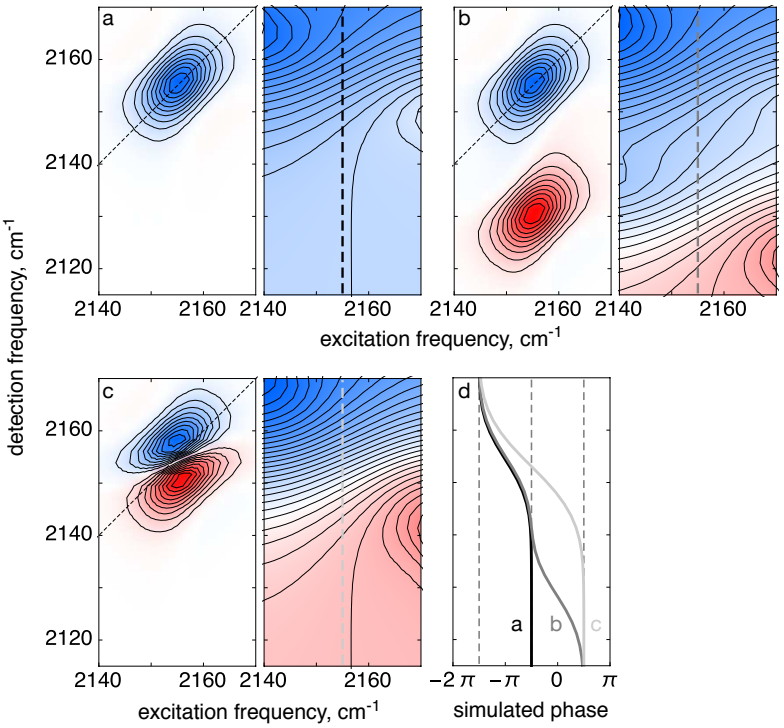

Fig. 1. Simulated purely absorptive 2D IR spectra (left) and associated phase profiles (right) as a function of anharmonicity ($\omega_{01} - \omega_{12}$) for (a) 250 cm^{-1}, (b) 25 cm^{-1}, (c) 2.5 cm^{-1}, representing three common classes of spectral response: fully isolated transitions, vibrations which overlap only minimally between the ground and excited state response, and significantly overlapping transitions where even the central frequencies of each transition overlap with the wings of other transition. d) Single frequency phase profiles along ω_1 = 2155 cm^{-1} are shown in a) black, b) grey, c) light grey, respectively. Dashed lines show phase values of $-3\pi/2$, $-\pi/2$, and $\pi/2$. Contours of the 2D IR spectra are shown at ±10% intervals of the signal maxima, while the phase profiles have contours drawn in steps of $\pi/10$ from -2π to 2π.

the ground state transition ranges from fully isolated to significantly overlapped with the excited state band.

In the case of the fully isolated transition (Fig. 1(a), where $\omega_{01} - \omega_{12}$ = 250 cm^{-1}, far from the 0–1 transition), a single bleach band is observed in the purely absorptive 2D IR spectrum in the frequency range of interest, and the associated phase profile varies smoothly along the detection frequency axis (taken along the linear absorption maximum of ω_1 = 2155 cm^{-1}) between $-3\pi/2$ to $-\pi/2$ across the band (Fig. 1(d), solid black line). At ω_3 = 2155 cm^{-1} the phase has a value of $-\pi$, as required for the real part of the Fourier transform to yield a negative amplitude. The phase profile may be understood by considering the contributions of the dispersive component, offset by a phase of $\pi/2$ from the absorptive component, but which has zero contribution to the four-wave mixing signal precisely at the linear absorption maximum, with an associated sign change upon passing through this central frequency. These simulations are consistent with previous observations from both IR [18] and electronic [19] multidimensional spectra of isolated transitions.

Optics EXPRESS

When the anharmonicity is $\omega_{01}-\omega_{12} = 25\ \mathrm{cm}^{-1}$, as in Fig. 1(b), the purely absorptive spectrum shows two bands, a bleach response identical to the previous case described above, and now with an excited state absorption band offset along ω_3 by $-25\ \mathrm{cm}^{-1}$, having the opposite sign of the bleach response. The associated phase profile shows similar features for the bleach transition, but the additional response from the excited state absorption band extends the modulation of the phase profile along ω_3 (see Fig. 1(d), grey line). The ESA response results in a second smoothly varying transition from $-\pi/2$ to $\pi/2$ across the ESA band, with a phase of 0 rad at $\omega_3 = 2130\ \mathrm{cm}^{-1}$, the central frequency of the band. We note that this is again the requirement for a positive valued band in the Fourier domain.

When the anharmonicity is smaller than the linewidth of the individual transitions associated with the ground and excited states (Fig. 1(c), for $\omega_{01} - \omega_{12} = 2.5\ \mathrm{cm}^{-1}$), the two bands overlap and, as a result, the individual lineshapes are significantly distorted. A similar distortion is observed in the associated phase profile, where the individual smoothly varying transitions are no longer resolved, and the phase values at the central frequencies of the transitions are no longer straightforwardly $-\pi$ and 0 rad as a result of the significant spectral overlap (Fig. 1(d), light grey line). However, the limits of the phase values remain the same, varying continuously from $-3\pi/2$ to $\pi/2$ across the entire detection frequency range associated with the four-wave mixing signal.

The above simulations thus give a distinct phasing target, that of the phase limits of $-3\pi/2$ to $-\pi/2$ for the ground state transition, or to $\pi/2$ if an excited state absorption band is also present, along the detection frequency axis at ω_1 equal to the central frequency of the transition. Experimental phase offsets are thus expected to merely shift the experimentally measured phase profiles by a constant value, which can be readily recovered from the experimental data.

3.2. Experiments

3.2.1. MeSCN

Multidimensional infrared spectra of MeSCN in DMF were measured at waiting times of $t_2 = 250$ fs, and 1, 10, and 20 ps. Total measurement time per 2D spectrum was ~2.5 minutes, where good signal to noise was achieved as a result of excellent laser stability and the fast scanning mechanical delay stages.

Without prior knowledge of the global phase correction which must be applied to recover purely absorptive 2D spectra, only the power spectral response can be visualized without phase ambiguity. As can be seen for the $t_2 = 250$ fs power spectrum (see Fig. 2(a)), two clear peaks are present, one centred at the excitation and detection frequency of $2155\ \mathrm{cm}^{-1}$, attributed to bleach and stimulated emission between the ground and first excited state, and a second peak which is redshifted along the detection frequency axis to $\sim 2130\ \mathrm{cm}^{-1}$, corresponding to excited state absorption to the second excited state. The associated phase spectrum (Fig. 2(b)) displays similar features as the simulated spectrum of Fig. 1(b), where the phase profile exhibits rapid change along the detection frequency axis at spectral positions corresponding to the bands observed in the power spectrum.

Quantitative comparison between the simulated and experimental phase profiles are shown in Fig. 2(c), with experimental data as black data points and the simulated phase profile from Fig. 1(b) is shown as a solid grey line. Excellent agreement between the experiment and simulated response are observed, where the phase profiles show effectively identical features. A constant offset of $\Delta\phi \approx 0.45\pi$ is observed between the experiment and simulated response, representing the global phase offset which arises due to imperfect control and knowledge of the relative delays and absolute phases of the excitation pulses used in the experiment. Strictly speaking, such a time-delay causes a frequency dependent phase, however, owing to our procedure of initial zeroing described in §2.2 [7], we make sure that this delay time is less than a light cycle, in which case the phase error can be approximated as one universal (frequency-independent) phase correction factor. That is, we perform the Fourier transforms in analogy to Eq. (3) and calculate

Optics EXPRESS

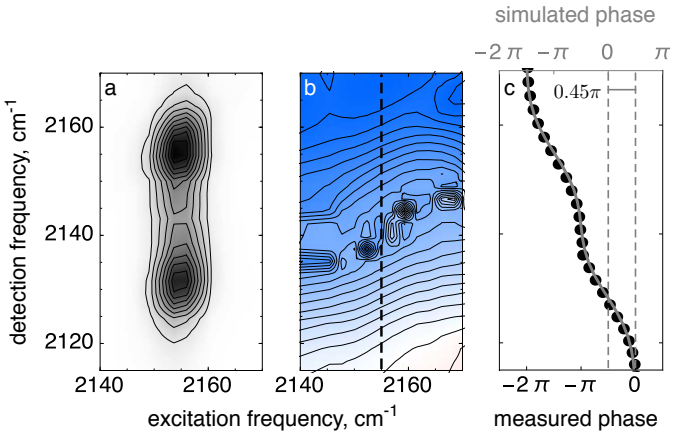

Fig. 2. Direct phasing of heterodyne-detected 2D IR spectra of MeSCN in DMF. a) Power spectrum and b) the associated phase spectrum (right) of the $t_2 = 250$ fs 2D response of the thiocyanate stretch vibration. From the power spectrum, ground and excited state transitions are observed separated along $\omega_3 = -25$ cm^{-1}. Contour lines are drawn at 10% intervals of the maximum amplitude of the power spectrum, and at intervals of $\pi/10$ between $\pm 2\pi$ for the phase spectrum. The discontinuities near the centre of the phase spectrum arise due to the near-zero amplitude of the experimental response along the nodal line between the ground and excited state transitions. c) The phase profiles through $\omega_1 = 2155$ cm^{-1} for both the experimental data (black points, bottom axis) and from the simulated 2D response with an anharmonicity of 25 cm^{-1} (grey line, top axis, taken from Fig. 1(b)), showing the excellent agreement between the theoretical and experimental phase profiles through the central frequency of the thiocyanate stretch vibration. A constant offset of $\Delta\phi \approx 0.45\pi$ is observed between the experimental and simulated spectra, and represents the global phase offset which must be corrected to generate the absorptive and dispersive 2D spectra.

the 2D spectrum as:

$$S_A(\omega_1, t_2, \omega_3) = \Re\left[e^{-i\Delta\phi}\left(S_R(-\omega_1, t_2, \omega_3) + S_{NR}(\omega_1, t_2, \omega_3)\right)\right] \tag{6}$$

and the corresponding phase spectrum

$$S_P(\omega_1, t_2, \omega_3) = \mathrm{Arg}[S_R(-\omega_1, t_2, \omega_3) + S_{NR}(\omega_1, t_2, \omega_3)] - \Delta\phi. \tag{7}$$

The phase correction $\Delta\phi$ is determined such that the phase varies from $-3\pi/2$ to $\pi/2$ along the detection frequency.

The result of the application of this phasing methodology is shown in Fig. 3 for all four waiting times, each phased independently. At early waiting times ($t_2 = 250$ fs and 1 ps) the purely absorptive 2D spectra reveal inhomogeneous broadening along the diagonal which persists beyond a waiting time of 1 ps. For long waiting time delays ($t_2 = 10$ and 20 ps) the lineshape becomes symmetric, revealing a homogeneous response as a result of spectral diffusion. In all cases we observe no mixing of absorptive and dispersive lineshapes, and the correlation of the central bleach frequency along the diagonal further indicates that the spectra are correctly phased. We note that for the reliable application of this technique at early waiting times, where inhomogeneous broadening affects the phase profiles, it is critical to correctly isolate the phase along the the central excitation frequency of the vibration of interest, as we observe offsets of up to $\pm 0.1\pi$ when extracting the phase profiles ± 2.3 cm^{-1} (± 1 pixel) about the central frequency.

Optics EXPRESS

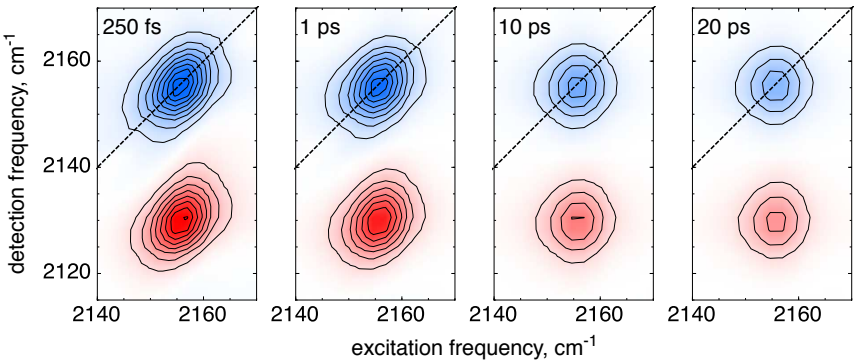

Fig. 3. Purely absorptive 2D IR spectra of MeSCN in DMF at select waiting times (indicated top left), directly phased as outlined in Fig. 2. Inhomogeneous broadening is observed at early waiting times, but on a 10 ps timescale the transition displays a homogeneous response as a result of spectral diffusion. Contours are drawn at ±10% intervals of the signal maximum of the t_2 = 250 fs spectrum.

The central excitation frequency can be read off from the power spectrum Fig. 2(a) without any ambiguity, i.e., before phasing.

3.2.2. Azidohomoalanine

This phasing methodology will be most useful in the case of low concentration limits for vibrations of interest where comparative methods, such as those based on the projection-slice theorem [3–5], will necessarily fail. A compelling example of this is the application of unnatural amino acids (UAAs) which have been designed with primarily either nitrile or azido reporter groups to give site-specific information on structure and dynamics of proteins through frequency shifts and spectral dynamics as a result of folding or function [14,20,21]. As most protein systems aggregate at concentrations >1 mM, the relative extinction coefficients and concentrations of the unnatural amino acid and water-based (either with hydrogen or deuterium) solvents results in the UAA response being buried in a significant solvent background [14, 22, 23]. Subsequent measurements of sample and buffer blanks are thus required to isolate the UAA signal of interest. We have learned that accurate phasing of both measurements independently is absolutely necessary for the complete subtraction of the solvent response. That is, even minor phase drifts in the order of 0.02π between the two measurements would severely affect the quality of the UAA spectra, and hence, the accurate determination of the central frequency of the reporter vibration of interest, where small frequency shifts on the order of 5–10 cm^{-1} report on the local protein environment.

The 2D IR response of a 100 μM azidohomoalanine sample in D_2O-based solvent is dwarfed by the solvent response, where the ~2120 cm^{-1} azido stretch vibration is effectively not visible (Fig. 4(a)). The azido band is sitting on a broad background [14, 24] originating from the excited state absorption of the OD stretch vibration of the D_2O buffer, where the fundamental of this transition can still be excited in the very red wing of the band [25] with the pump pulses, centered at 2110 cm^{-1}, used for this experiment. The associated phase response (Fig. 4(b)), which is essentially flat over the spectral window of interest, originates exclusively from the water background, since the contribution of the Aha azido group to the overall detected signal is miniscule. A critical step for the subtraction of the buffer response from these data is the relative alignment of the time domain response, which we perform by correcting for the average

Optics EXPRESS

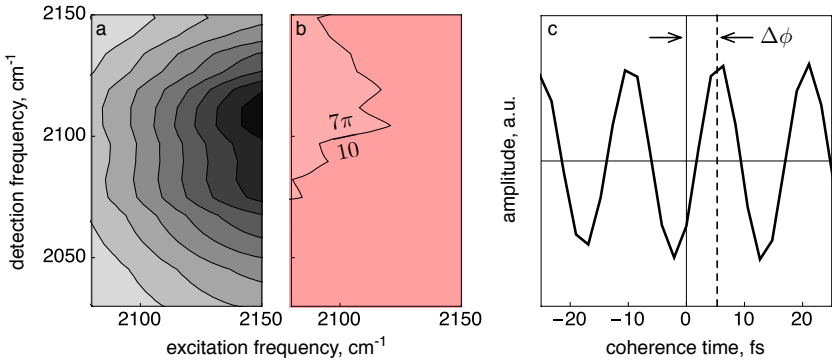

Fig. 4. Alignment of time domain interferograms based on solvent response. The (a) power spectrum (contours drawn at 10% intervals of the maximum amplitude) and b) phase profile (contours drawn in steps of $\pi/10$) of 100 μM Aha in D_2O solvent, where the response is dominated by a broad solvent background which spans the entire spectral domain of interest. The phase profile in particular shows an effectively flat phase in the spectral region of interest, and can thus be used to align subsequent measurements. This is realized through spectral integration of the time domain signals across the detection frequency range of the spectrometer to give the highest signal to noise for the determination of the phase, where c) the phase offset of $\sim 0.7\pi$ is visible in the spectrally-integrated response. The phase of $\sim 0.7\pi$ represents the *per se* unknown phase of the water background in addition to the imperfect control and knowledge of the relative phases of the excitation pulses. Rolling the time domain signals by the negative of this net phase offset in the Fourier domain allows for individual alignment of each set of time-domain interferograms seperately.

phase offset over the spectral window shown in Fig. 4(b) for the Aha measurement and for the buffer measurements independently. This procedure uses the *per se* unknown phase of the water background as a reference, resulting in an accurate subtraction of the solvent response. The isolated Aha signals of interest can then be phased using the fixed phase limits as described previously.

The accurate phasing of the isolated Aha response is shown in Fig. 5, where the power spectrum of the isolated Aha signal (Fig. 5(a)) shows an excitation frequency maximum of $\omega_1 = 2120\ \text{cm}^{-1}$. The phase profile associated with this excitation frequency is shown in Fig. 5(b), where the experimental phase offset after correcting for the phase offset of the large D_2O response is approximately $\sim 0.11\pi$. Correction for this offset produces the 2D spectrum shown in Fig. 5(c), where the bleach and excited state absorption shown a roughly 2:1 intensity ratio, and an assurance of good phasing is indicated by the correlation of the bleach maximum along the diagonal.

It is by coincidence that the phase of the D_2O-based solvent response in this spectral region exhibits a flat profile, which results in an excellent signal to noise for the initial alignment of the time-domain interferograms to facilitate background subtraction. In a different spectral region, or for H_2O-based solvents [25, 26], the specific phase profiles will vary greatly, but the general methodology will still apply given any reference signal with sufficient signal to noise over which to align subsequent measurements. The global phase offset can then be recovered from the solute vibration of interest via the fixed phase limits identified herein, making this a generally applicable scheme for the phasing any isolated vibrational mode or for vibrational modes buried in a strong solvent response. Indeed, the calibration of this constant residual phase offset from the solvent response in a given frequency window, as determined above for Aha in D_2O-based solvent, allows for direct phasing of any subsequent 2D signals from the solvent response directly.

Optics EXPRESS

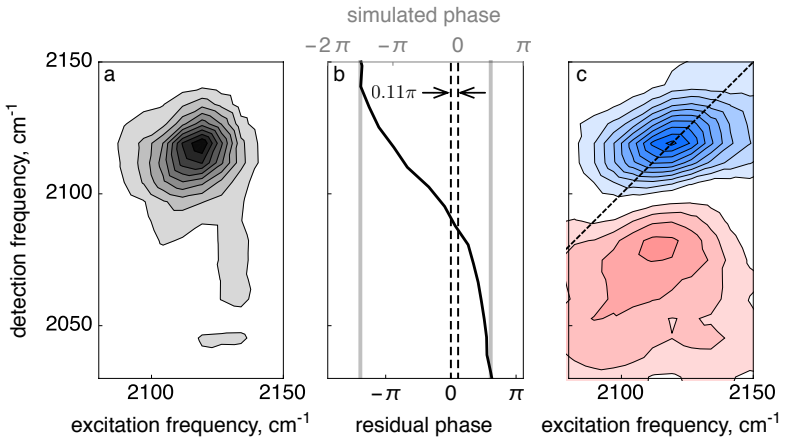

Fig. 5. Phasing the isolated Aha response. a) The power spectrum of the Aha response following background subtraction in the time domain. The central excitation frequency of the power spectrum is observed to be at ~2120 cm^{-1}. b) The experimental phase profile at $\omega_1 = 2120\ cm^{-1}$, showing the characteristic progression between fixed phase limits of $[-3\pi/2, \pi]$ across the detection frequency window associated with the power spectral response. A residual offset of $\sim 0.11\pi$ is observed between the experimental phase of the Aha response and the expected fixed phase limits from the simulated response. Correction of this phase offset leads to c) the purely absorptive spectrum of Aha without phase ambiguity, showing 0–1 and 1–2 transitions with an amplitude ratio of ~2:1. Contours are drawn in steps of ±10% the signal maximum.

4. Conclusion

Two-dimensional IR spectroscopy began as a frequency domain measurement with a narrowband pump-broadband probe pulse sequence [12], where the self-heterodyned nature of transient absorption spectroscopy had no phase ambiguity. The technique rapidly advanced to become a Fourier-transform technique involving four pulses in a boxcar geometry, which allowed for better signal to noise and higher temporal resolution, but at a cost of simplicity in experimental design and use. Although methods were developed to allow for the recovery of the purely absorptive vibrational response in boxcar geometry multidimensional spectroscopy [3–8], most modern implementations of 2D IR spectroscopy combine the Fourier transform approach with a more straightforward pump-probe geometry [9, 27–29], greatly simplifying the phasing problem as a result of collinear pump pulses and a self-heterodyned probe pulse.

The boxcar geometry, however, still yields the highest possible sensitivity for the collection of multidimensional IR spectra, and in extending the technique to ever lower concentrations and to weaker absorbers [24], methods to enhance the reliability of phasing and ease of use of boxcar geometry 2D IR are still of great importance. The present phasing methodology based on analysis of the heterodyne-detected signals themselves thus represent an important first step in bringing the ease of use of pump-probe geometry 2D IR to boxcar geometry spectrometers. The approach requires no auxiliary measurements, allows for accurate phasing of spectra from samples of any thickness, and is insensitive to long-term drift of the interferometer. As a result, this phasing procedure allows for the determination of purely absorptive multidimensional vibrational spectra at the lowest limits of detectability.

Optics EXPRESS

Funding

This work has been supported in part through a European Research Council (ERC) Advanced Investigator Grant (DYNALLO) and in part through the Swiss National Science Foundation through the National Center of Competence and Research (NCCR) MUST.

Acknowledgments

We thank Jan Helbing for helpful discussions and for the simulation code.